# Structural Basis for the Self-Chaperoning Function of an RNA Collapsed State†

Ivelitza Garcia and Kevin M. Weeks*

*Department of Chemistry, University of North Carolina, Chapel Hill, North Carolina 27599-3290*

*Received June 30, 2004; Revised Manuscript Received September 15, 2004*

ABSTRACT: Prior to folding to a native functional structure, many large RNAs form conformationally collapsed states. Formation of the near-native collapsed state for the bI5 group I intron RNA plays an obligatory role in self-chaperoning assembly with its CBP2 protein cofactor by preventing formation of stable, misassembled complexes. We show that the collapsed state is essential because CBP2 assembles indiscriminately with the bI5 RNA in any folding state to form long-lived complexes. The most stable protein interaction site in the expanded state−CBP2 complex overlaps, but is not identical to, the native site. Folding to the collapsed state circumvents two distinct misassembly events: inhibitory binding by multiple equivalents of CBP2 and formation of bridged complexes in which CBP2 straddles cognate and noncognate RNAs. Strikingly, protein-bound sites in the expanded state RNA complex are almost the inverse of native RNA−RNA and RNA−protein interactions, indicating that folding to the collapsed state significantly reduces the fraction of RNA surfaces accessible for misassembly. The self-chaperoning function for the bI5 collapsed state is likely to be conserved in other ribonucleoproteins where a protein cofactor binds tightly at a simple RNA substructure or has an RNA binding surface composed of multiple functional sites.

Significant recent work emphasizes that most (*1*−*6*), but not all (*7*), large RNAs fold rapidly (*8*−*11*) to compact, but not quite native, structures under roughly physiological ion environments. Collapsed states are thermodynamically dominant for several nascent large RNAs that function in the cell solely as complexes with obligate protein cofactors, including the bI5 and bI3 group I introns and domains of *Escherichia coli* 16S RNA (*1*, *12*). Rapid formation of collapsed states for these large RNAs is likely to be fundamental to their ribonucleoprotein (RNP) assembly reactions.

Prior to binding by its obligate (*8*, *13*) CBP2 protein cofactor, the catalytic core of the bI5 RNA forms a collapsed state. As dictated by the Boltzmann distribution, the collapsed (and native) state must sample both extended and native-like conformations. On average, however, as judged by mapping structural neighbors in three-dimensional space, the global structure of the collapsed state lies very near to that of the native structure but is sufficiently relaxed or dynamic to be almost uniformly solvent accessible (*1*, *4*, *8*) (see collapsed state in Figure 1). CBP2 consolidates the final phase of RNA folding (*4*) by binding (i) to the catalytic core at the stacked P3−P8 and P7.1−P7.1a helices and (ii) to the P2 helix and J2/3 structure that links the 5′ domain and catalytic core (see N·CBP2 structure, Figure 1). The global structure of the bI5 RNA can be manipulated by varying the $Mg^{2+}$ concentration: at 7 mM, the collapsed state predominates, whereas at 0 mM the poorly folded expanded state is favored (Figure 1).

The effectiveness of CBP2 as a protein cofactor is critically dependent on the bI5 RNA conformation. If the RNA is in the near-native (*4*) collapsed state, CBP2 binding chases the RNA to the native state (pathway I in Figure 1). In contrast, CBP2 binding to the expanded state yields a kinetically trapped complex (E·CBP2 in Figure 1) that is structurally distinct from the native state by multiple criteria (*4*, *8*). The kinetically trapped complex could, in principle, resolve by either of two broad mechanisms: (i) CBP2 could dissociate and rebind to the productive collapsed RNA state or (ii) the kinetically trapped complex could undergo a unimolecular rearrangement to form the native complex (pathways IIa and IIb in Figure 1).

On-pathway intermediates in an RNP assembly reaction must, by definition (*4*, *8*), facilitate *native* RNP assembly. The bI5 RNA collapsed state is a productive, on-pathway, intermediate because only this state is chased to the native state upon protein binding (Figure 1). Analogous RNA collapsed states are likely to play essential roles in assembly of many RNPs.

## METHODS

*General.* Reactions were performed in 50 mM MOPS (pH 7.6), 50 mM KCl, and varying $MgCl_2$ concentrations at 35 °C, supplemented with $^1/_{10}$th volume of CBP2 in protein dilution buffer [20 mM MOPS (pH 7.6), 200 mM NaCl, 0.1 mM EDTA, 2 mM DTT, 1 mg/mL BSA, and 40% (v/v) glycerol]. RNAs were generated by in vitro transcription, 5′- or 3′-$^{32}$P-end labeled, and refolded as described (*14*).

*Equilibrium ($K_d$) and Kinetic ($k_{on}$, $k_{off}$) Binding Experiments.* Dissociation constants for CBP2 binding to the bI5 RNA as a function of $MgCl_2$ concentration (0−7 mM) were measured under conditions sufficient to achieve equilibrium (35 °C, 1 h) (*13*) by filter partitioning against dual nitrocellulose and anionic membranes using 5−50 pM $^{32}$P-labeled bI5 RNA. CBP2 concentrations required to precisely saturate

† We are indebted to NIH Grant GM56222 for financial support of this work.

* Corresponding author. Phone: 919-962-7486. Fax: 919-962-2388. E-mail: weeks@unc.edu.

10.1021/bi048626f CCC: $27.50 
Published on Web 11/10/2004

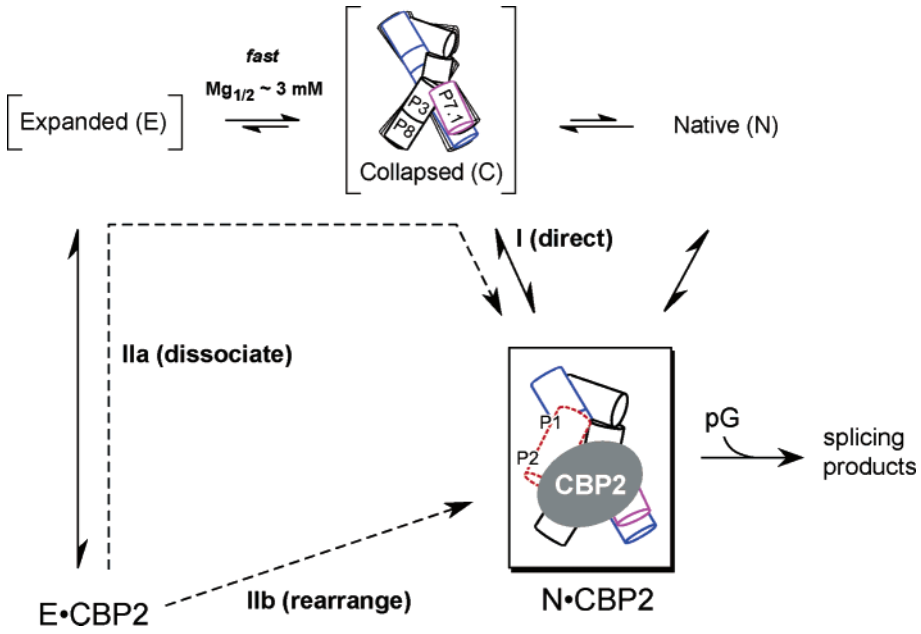


FIGURE 1: Self-chaperoning role of the bI5 RNA collapsed state for productive assembly with CBP2. Binding by CBP2 to the near-native (4) collapsed state (C) chases the bI5 RNA to the native ribonucleoprotein complex (N•CBP2; pathway I). CBP2 also binds to the expanded state RNA (E) to form a trapped complex (E•CBP2) that, in principle, could resolve to a productive RNP either by dissociation and rebinding or by rearrangement (pathways IIa and IIb).

RNA binding were determined in stoichiometric binding experiments (100 nM RNA, 7 mM $MgCl_2$). If added, low-affinity complexes were competed by 20 or 100 $\mu$g/mL heparin. Association and dissociation rates were determined by trapping free CBP2 with heparin and detecting the fraction of RNA bound by dual filter partitioning (*15*).

*Splicing Kinetics and $Mg^{2+}$ Jumps.* Reactions (50 $\mu$L) were generally performed with 6 nM 5′-$^{32}$P-end-labled bI5 RNA and 7 nM CBP2. Precursor RNA was refolded [in reaction buffer at 0, 3, or 7 mM $MgCl_2$, 35 °C (*8*)] prior to addition of CBP2 and incubated for 10 min. Splicing experiments were simultaneously jumped to 7 mM $Mg^{2+}$ and initiated by diluting reactions 2-fold with reaction buffer supplemented with pG (to 2 mM final). Aliquots were quenched with formamide/EDTA gel loading solution and resolved on 8% denaturing polyacrylamide gels. Lag kinetics, if observed, were fit to an expression for consecutive, irreversible reactions, fraction reacted $(F_2) = A(k_1 - k_2)^{-1}[k_2 \exp(-k_1 t) - k_1 \exp(-k_2 t)] + (1 - A)$ (*8*), where $k_1$ and $k_2$ are rate constants for the two steps and $A$ is the fraction of reactive RNA. Competitors were 20 $\mu$g/mL heparin, 500 nM unlabeled bI5 RNA, or 900 $\mu$g/mL total yeast RNA (Sigma-Aldrich).

*Phosphorothioate Footprinting.* Complexes were formed using 10 nM 5′- or 3′-end-labeled phosphorothioate-substituted bI5 RNA (*14*) and 60 nM CBP2; if added, the heparin concentration was 20 $\mu$g/mL. RNA phosphorothioate linkages were cleaved by addition of $^1/_{10}$th volume of freshly prepared 1 mM iodine (in water), quenched after 20 s by addition of 2-mercaptoethanol to 50 mM, and resolved by denaturing electrophoresis (*14*). Normalized cleavage efficiencies ≤80% or ≥120% were scored as protection and enhancement, respectively.

## RESULTS

*CBP2 Assembles Indiscriminately with Expanded and Collapsed RNA States.* Even though the CBP2 interaction site on the native bI5 RNA can only form in the context of the correct RNA tertiary structure (boxed structure in Figure 1), the protein does bind tightly to the RNA independent of whether the RNA is in the expanded, collapsed, or native states (*8*). We, therefore, explored the possibility that CBP2 discriminates against the expanded state by binding more rapidly to the more structured collapsed and native states. We monitored time-dependent RNP assembly and disassembly by nitrocellulose filter binding (*13*, *14*). Protein binding was quenched by addition of the nonspecific competitor heparin, which means that only stable RNP complexes are scored.

When CBP2 is added to the collapsed state RNA (at 7 mM $Mg^{2+}$), a larger fraction of RNA is bound with increasing CBP2 concentrations at long time points, as expected, until the protein concentration sufficiently exceeds the equilibrium dissociation constant ($K_d$) (Figure 2A, top panel). Consistent with prior work (*8*, *15*, *16*), the bimolecular CBP2−RNA complex forms with distinctive kinetics such that the association rate constant, 0.5 ± 0.1 $min^{-1}$, is independent of protein concentration over a broad range (solid lines, Figure 2A). Thus, some unimolecular event governs overall assembly (*15*). If this characteristic unimolecular step requires formation of the collapsed state, then CBP2 association kinetics might be different for assembly with the expanded state RNA.

Unexpectedly, assembly of CBP2 with the expanded state (in the absence of $Mg^{2+}$) follows kinetics identical to those observed for assembly with the collapsed state (compare upper and lower panels in Figure 2A). Association rates, 0.33 ± 0.08 $min^{-1}$, are independent of protein concentration over the range 0.5−20 nM CBP2. When assembly is monitored at 3 mM $MgCl_2$, where the expanded and collapsed states are roughly equally populated (*1*, *4*), observed rates (0.38 ± 0.04 $min^{-1}$) remain independent of CBP2 concentration.

Assembly rate constants measured under $Mg^{2+}$ environments that stabilize distinct population ratios of the expanded

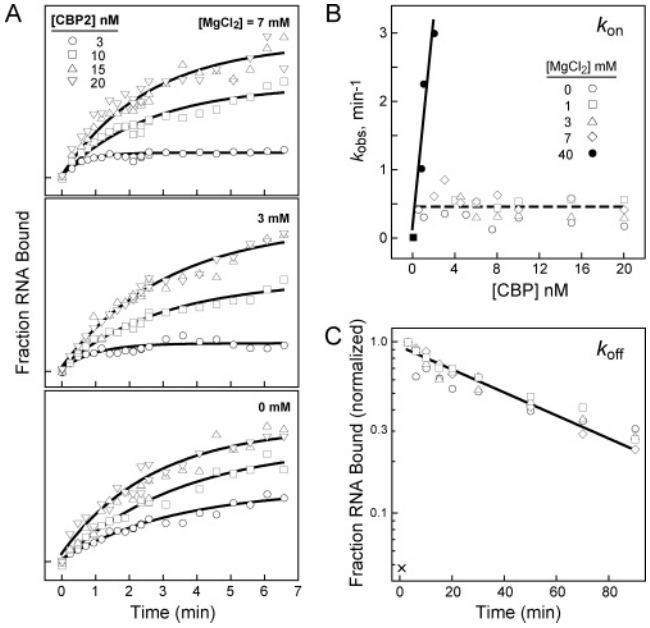


FIGURE 2: CBP2 cannot discriminate between collapsed and expanded state RNAs. (A) Assembly of the CBP2−bI5 RNA complex at the indicated CBP2 concentrations at 7, 3, and 0 mM $MgCl_2$. Rates were obtained by fitting to a single exponential (solid lines). The fraction of RNA retained on the filter at saturating protein concentration varied from 0.4 to 0.6 for the individual series of experiments shown. (B) Rate constants obtained in individual assembly experiments plotted as a function of CBP2 concentration. Rate-limiting unimolecular versus bimolecular processes are shown with open and closed symbols, respectively. (C) Disassembly of CBP2−bI5 RNA complexes. Symbols for [$MgCl_2$] are the same as in panel B. Dissociation rate constants are $0.016 \pm 0.003$ $min^{-1}$, in all cases (solid line). Addition of the heparin competitor prior to protein (×) yields a background retention of <5%.

and collapsed state RNAs are summarized in Figure 2B (open symbols) and show that some (protein concentration independent) unimolecular process governs assembly of the bI5 RNP complex, independent of whether the RNA is in the collapsed or expanded state or in a mixture of these states.

The above assembly behavior was compared to association of CBP2 with the bI5 RNA at 40 mM $Mg^{2+}$, where the RNA catalytic core is predominantly in the native state (*1*, *4*, *8*, *15*). At 40 mM $Mg^{2+}$, CBP2 binds with true second-order behavior and a rate constant ($k_{on} = 2 \pm 1 \times 10^9$ $M^{-1}$ $min^{-1}$; solid symbols, Figure 2B) consistent with diffusion-limited assembly.

To determine if complexes between CBP2 and the expanded and collapsed states can be discriminated on the basis of different lifetimes, we monitored disassembly of complexes preformed at $MgCl_2$ concentrations ranging from 0 to 7 mM. The measured dissociation rate constant for all CBP2−bI5 RNA complexes is $0.016 \pm 0.003$ $min^{-1}$, corresponding to a half-life of 50 min (Figure 2C). The rate of disassembly is thus independent of whether the RNA is in the expanded or collapsed state. Slow complex disassembly also means that (at least 1 equiv of) CBP2 remains bound to the bI5 RNA as the RNA folds from the expanded to the native conformation (pathway IIb in Figure 1).

This initial kinetic analysis supports two important conclusions. First, CBP2 is incapable of discriminating between the expanded and collapsed states during either RNP assembly or RNP disassembly. Second, CBP2 assembly behavior changes from a slow unimolecular to a rapid bimolecular (second-order) process when conditions favor the native bI5 core structure (compare dashed and solid lines in Figure 2B), strongly supporting a previous model (*15*) postulating that a unimolecular RNA conformational change is rate limiting for overall RNP assembly. The new observation (Figure 2A) that first-order association kinetics are observed with both the expanded and collapsed states suggests that a similar rate-limiting step governs assembly of CBP2 with either RNA state.

*Dual CBP2 Binding Modes with the Expanded State RNA.* The experiments outlined above demonstrate that both CBP2 assembly with and disassembly from the RNA expanded state are kinetically indistinguishable from those for the collapsed state. Binding kinetics thus cannot explain the productive, self-chaperoning, function of the collapsed state. We, therefore, sought to identify whether an additional (nonproductive) binding mode exists for CBP2 that is specific to the expanded state. Initially, binding constants were measured for CBP2 complexes with the expanded and collapsed state RNAs in the presence and absence of the competitor heparin, using filter partitioning (Figure 3A).

For RNA−protein complexes formed at 7 mM $MgCl_2$, where CBP2 binding chases the RNA to the native state (Figure 1), addition of heparin after formation of the complex had no significant effect on binding ($K_d$'s = 1.4−2.0 nM; closed symbols, Figure 3A). The absence of a heparin effect is consistent with slow complex dissociation (Figure 2C). In contrast, CBP2 binds tightly to the expanded RNA (0 mM $Mg^{2+}$) state ($K_{1/2} = 0.36$ nM; open circles, Figure 3A) with a binding isotherm in the absence of heparin that systematically deviates from a one protein−one RNA binding profile (the observed positive cooperative binding has a Hill coefficient of ~1.8; see dashed line in Figure 3A). When heparin is added immediately prior to filter partitioning, the apparent $K_d$ increases by 8-fold to 2.7 nM and the resulting binding profile fits a simple stoichiometric binding relationship (compare open circles and squares in Figure 3A). Thus, CBP2 binds tightly to the expanded state RNA via both competitor-resistant and competitor-sensitive modes.

We then tested whether multiple binding modes contribute to the formation of the nonproductive CBP2−expanded state RNA complex. In these splicing experiments, CBP2 was allowed to bind to either the expanded or collapsed state at defined [CBP2]/[RNA] ratios. This state is denoted as $X^{CBP2}$, where X is the initial [$MgCl_2$]. Preformed complexes were then jumped to 7 mM $MgCl_2$ and 2 mM guanosine 5′-monophosphate (pG) nucleophile concentrations (denoted by →splicing in Figure 3B), which support splicing (*8*, *13*) (Figure 1). When CBP2 is preincubated with the collapsed state RNA (7 mM $Mg^{2+}$), addition of a saturating concentration of pG leads to efficient splicing (rate ~2 $min^{-1}$) independent of whether CBP2 is present at equal molar or superstoichiometric concentrations (up to 5-fold excess) relative to the bI5 RNA concentration (solid circles, Figure 3B).

In contrast, splicing kinetics for the CBP2−expanded state RNA complex are strongly sensitive to whether CBP2 is in excess. When the CBP2 concentration is 5-fold higher than the expanded state RNA concentration [at 6 nM (0 mM $Mg^{2+}$)] prior to a 7 mM $Mg^{2+}$ and pG jump (a $0^{CBP2}$ → splicing experiment), the onset of splicing is delayed by a distinct lag (▲ in Figure 3B). This lag phase profile is

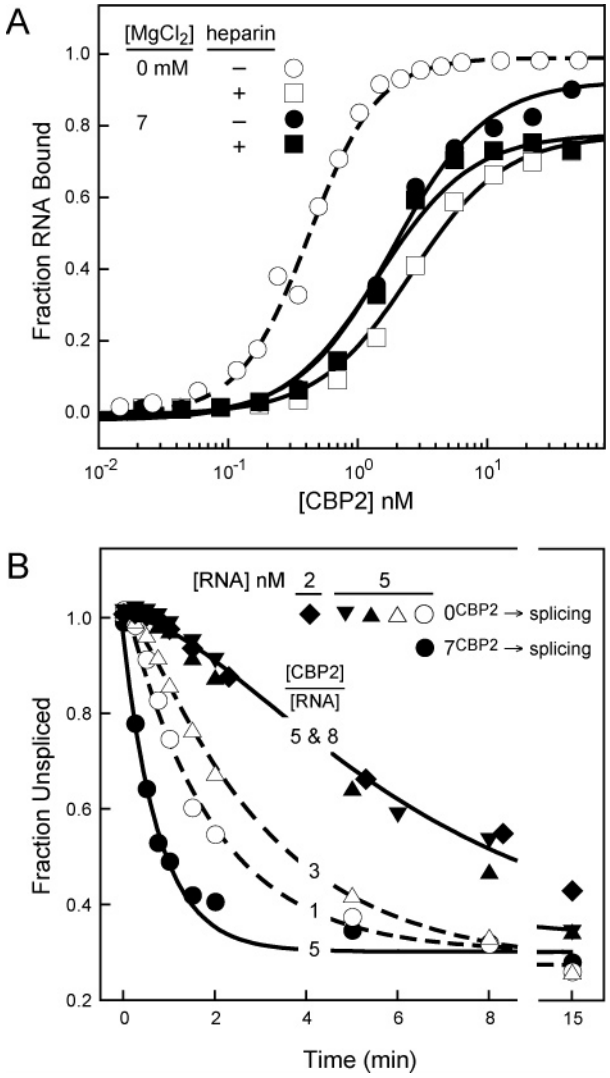


FIGURE 3: Dual CBP2 binding modes with the expanded state RNA. (A) Equilibrium binding by CBP2 to the expanded and collapsed state RNAs (0 and 7 mM $MgCl_2$, respectively). In the absence of competitor (circles) observed equilibrium dissociation constants ($K_d$) are 0.3 and 2 nM. CBP2 binding in the absence of divalent ion shows a modest cooperativity (Hill coefficient 1.8, dashed line). Upon addition of heparin, the apparent $K_d$ at 0 mM $MgCl_2$ increases to ~3 nM (open squares). (B) Multiple CBP2 binding events trap the expanded state RNA in a complex that rearranges slowly to the native state. When either a 5- (◆, ▲) or 8-fold (▼) excess of CBP2 is incubated with the RNA (at 2 or 5 nM) in the absence of divalent ion, $0^{CBP2}$, and then jumped to 7 mM $MgCl_2$ to allow splicing (→splicing), a distinct kinetic lag is observed. The two kinetically significant steps have rate constants of 0.2 and 0.5 $min^{-1}$. The lag phase is reduced (open triangles) or eliminated (open circles) as the [CBP2]/[RNA] ratio approaches 1.

consistent with a reaction governed by two rate-determining steps with rate constants of 0.2 and 0.5 $min^{-1}$. The 5-fold excess of CBP2 is sufficient to saturate the inhibitory effect because increasing the CBP2 concentration to 8-fold over RNA does not further increase the lag phase [compare [CBP2]/[RNA] ratios of 5 (▲) and 8 (▼) in Figure 3B]. An identical profile is also obtained when the RNA concentration is reduced to 2 nM (approximately equal to the $K_d$) in the presence of 5 equiv of CBP2 (see ◆ in Figure 3B).

The inhibitory effect of CBP2 binding is reduced at lower stoichiometric ratios of protein (see 3-fold excess CBP2 reaction; open triangles in Figure 3B). At an equimolar protein−RNA ratio, splicing proceeds with the rate of 0.5 (±0.1) $min^{-1}$ without an apparent lag phase (open circles, Figure 3B). Thus, we infer that the second slower step (0.2 $min^{-1}$), observed only at superstoichiometric protein ratios, reflects dissociation of nonproductively bound CBP2 equivalents. The ability of the protein cofactor to interact with the bI5 RNA in this inhibitory fashion is a feature tightly linked to CBP2's intrinsic properties since both binding modes are characterized by similar overall binding constants (compare splicing experiments performed at 2 and 5 nM RNA; ◆ and ▲ in Figure 3B).

*Two RNA Binding Surfaces for Specifically Bound CBP2.* The observation that a single equivalent of CBP2 dissociates slowly (Figure 2C) and is sufficient to promote splicing of the expanded state RNA upon jumping to 7 mM $MgCl_2$ (open circles in Figure 3B) strongly suggests that the kinetically trapped RNP complex is resolved, in part, by a rearrangement mechanism (pathway IIb in Figure 1). Moreover, the RNA recognition surface of CBP2 potentially also undergoes a change in local structure during the protein-bound rearrangement to the native state. We, therefore, tested whether folding from the expanded to the native state RNA, as a complex with CBP2, is sensitive to the addition of a competitor capable of disrupting the ability of CBP2 to form *new* RNA contacts (illustrated schematically in Figure 4A).

In these structure-competition experiments, CBP2−bI5 RNA complexes were preformed at 0, 3, or 7 mM $MgCl_2$ and equimolar RNA and protein concentrations (denoted as $X^{CBP2}$, where X is the initial [$MgCl_2$]). Subsequently, a competitor (heparin, bulk yeast RNA, or bI5 RNA) was added to the reaction (denoted by $\rightarrow X^{CBP2}_{COMP}$) and splicing initiated by the simultaneous addition of pG and $MgCl_2$ to 7 mM (indicated with →splicing) (Figure 4A). An experiment in which a complex is preformed at 0 mM $Mg^{2+}$, challenged with a competitor, and then jumped to 7 mM $MgCl_2$ to initiate splicing is thus indicated by $0^{CBP2} \rightarrow 0^{CBP2}_{COMP} \rightarrow$ splicing.

As a control, splicing was first monitored without the competitor-addition step. When CBP2 is added to the bI5 RNA at 7 mM $MgCl_2$, binding by the protein chases the RNA to the native state (pathway I in Figure 1) and yields a splicing rate of 2.6 ± 0.3 $min^{-1}$ ($7^{CBP2} \rightarrow$ splicing; closed circles in Figure 4B). For complexes preformed at 0 mM $MgCl_2$, the splicing profile is characterized by a single exponential at 0.5 ± 0.1 $min^{-1}$ ($0^{CBP2} \rightarrow$ splicing; open circles, Figure 4B). When complexes were preformed at 3 mM $MgCl_2$, where both expanded and collapsed RNA states are populated, we observe an intermediate splicing rate (1.2 ± 0.5 $min^{-1}$) with no detectable lag consistent with one fraction of RNA molecules, initially in the collapsed state, splicing at 2.6 $min^{-1}$ (~55%) and a second fraction, in the expanded state, splicing at 0.5 $min^{-1}$ (~45%) (see $3^{CBP2} \rightarrow$ splicing; triangles in Figure 4B).

Addition of any of the three competitors to labeled bI5 RNA at 7 mM $MgCl_2$ ($7_{COMP}$), *prior* to addition of CBP2 ($7_{COMP} \rightarrow 7^{CBP2}_{COMP} \rightarrow$ splicing; closed squares in Figure 4C), dramatically lowers the extent of splicing to less than 15% over 15 min, illustrating that all three competitors disrupt productive CBP2 binding. When the competitor is added *after* CBP2 at 7 mM $Mg^{2+}$ ($7^{CBP2} \rightarrow 7^{CBP2}_{COMP} \rightarrow$ splicing), splicing occurs at rates spanning 2.1−3.5 (± 0.3) $min^{-1}$ for

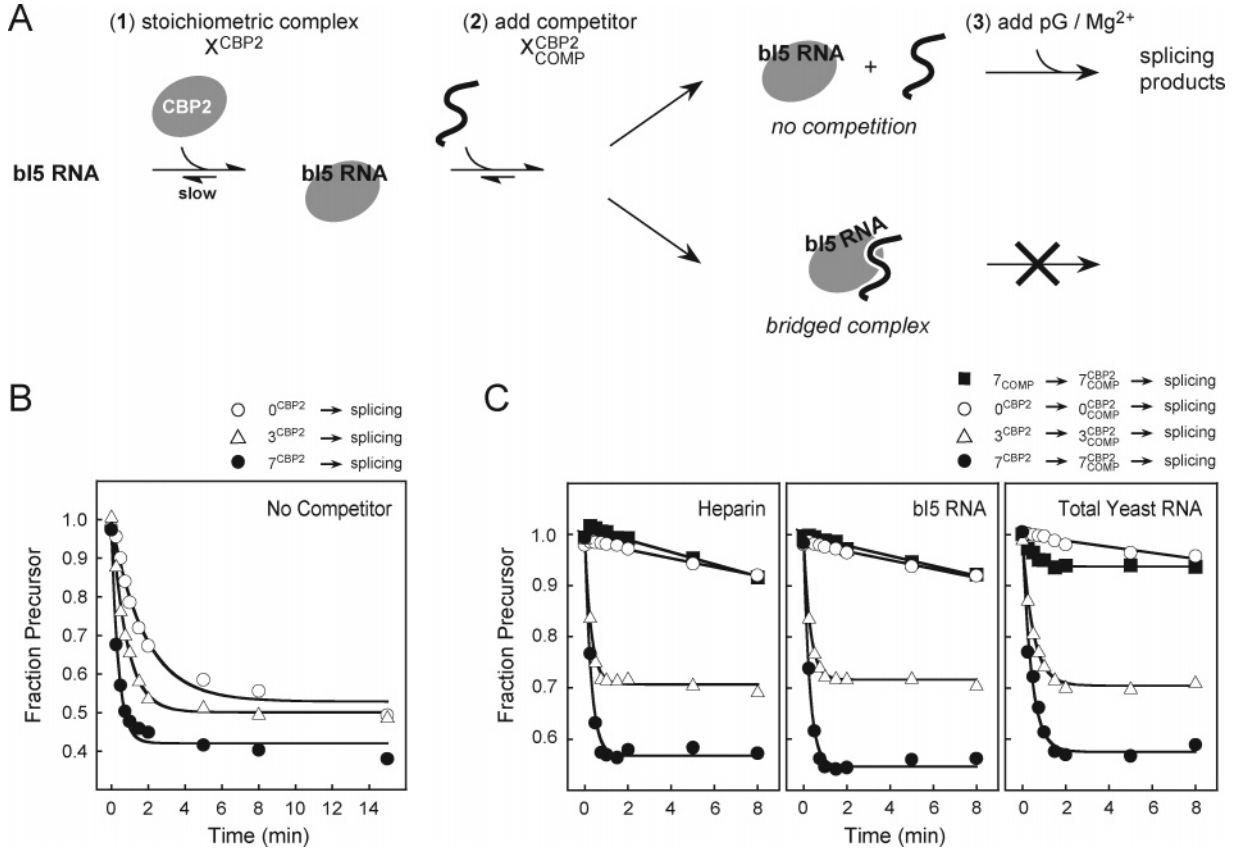


FIGURE 4: Inactivation of the CBP2−expanded state RNA complex via formation of bridged complexes with competitors. (A) Scheme for evaluating competitor-induced inactivation of CBP2−RNA complexes. Ribonucleoprotein complexes are (1) preformed at an initial [$MgCl_2$] ($X^{CBP2}$), (2) challenged with one of three competitors (heparin, bI5 RNA, or total yeast RNA; $X^{CBP2}_{COMP}$), and (3) allowed to splice by jumping to 7 mM $MgCl_2$ and adding pG (→splicing). Relative to splicing, complex dissociation is slow. (B) Control experiments without added competitor. (C) $Mg^{2+}$-jump reactions for each of three competitors. In prequench reactions ($X_{COMP}$), competitor is added prior to CBP2.

heparin, total RNA, and excess bI5 RNA (closed circles, Figure 4C). These rates are comparable to the rate measured in the absence of competitor (Figure 4B) and demonstrate that competitors do not disrupt preformed native complexes.

In strong contrast, when the competitors are added to the preformed RNA−protein complex at 0 mM $MgCl_2$ ($0^{CBP2} \rightarrow 0^{CBP2}_{COMP} \rightarrow$ splicing), 10% or less of the labeled bI5 RNA splices (open circles, Figure 4C). When experiments were performed with preformed RNA−CBP2 complexes at 3 mM $MgCl_2$, where both collapsed and expanded states are populated ($3^{CBP2} \rightarrow 3^{CBP2}_{COMP} \rightarrow$ splicing), approximately half of the complexes splice efficiently ($k_{obs}$ = 2.4−3.1 $min^{-1}$) while the other half splice poorly (open triangles, Figure 4C), consistent with the ratio of collapsed to expanded state RNAs *initially* in the reaction.

These data support the interpretation that CBP2-bound expanded state RNAs must form significant new CBP2−RNA contacts *prior* to splicing. Once correctly formed, these contacts are competitor-resistant. Because dissociation of the CBP2−RNA complex is slow (Figure 2C), addition of competitor yields a "bridged" complex involving CBP2, bI5 RNA, and competitor (Figure 4A).

*Structural Analysis of CBP2 Binding to the RNA Expanded and Collapsed States.* We identified structural differences between CBP2 complexes with the collapsed and expanded state RNAs using iodine-mediated phosphorothioate footprinting (*17*, *18*). We found that iodine-mediated cleavage is inert to the addition of heparin; thus, we can compare footprinting patterns for (i) CBP2 complexes with the expanded or collapsed state RNAs to (ii) complexes challenged with heparin. Footprinting patterns were obtained with RNAs sparsely substituted with each of the four phosphorothioate-substituted ribonucleotides. Cleaved RNAs were resolved in sequencing gels and banding patterns converted to plots of intensity versus position (representative data for A residues are shown in Figure 5A,B).

Cleavage patterns for free bI5 RNA at both 0 and 7 mM $MgCl_2$ are identical to that for RNAs treated with heparin prior to CBP2 addition (compare black and gray lines, Figure 5A,B). Thus, when added first, heparin completely eliminates CBP2 binding, as expected. Upon addition of CBP2 to the bI5 RNA at 0 or 7 mM $MgCl_2$, significant positions in the RNA become protected from cleavage or show enhanced cleavage (compare blue and black traces in Figure 5A,B). At the strongest protections (or enhancements), cleavage intensities differ by just over 2-fold. Even though the absolute magnitude of protection may be small, band intensities can be rigorously normalized to multiple, unperturbed bands and are thus reproducible over multiple, independently evaluated experiments. A comprehensive summary of RNA cleavage patterns is shown in Figure 5C,D.

When CBP2 is added to the collapsed state RNA (7 mM $MgCl_2$), the pattern of protection shows good agreement with prior hydroxyl radical footprinting experiments (*1*, *8*). Specifically, protein binding and RNA folding protect the RNA backbone from iodine-mediated cleavage in the P5−

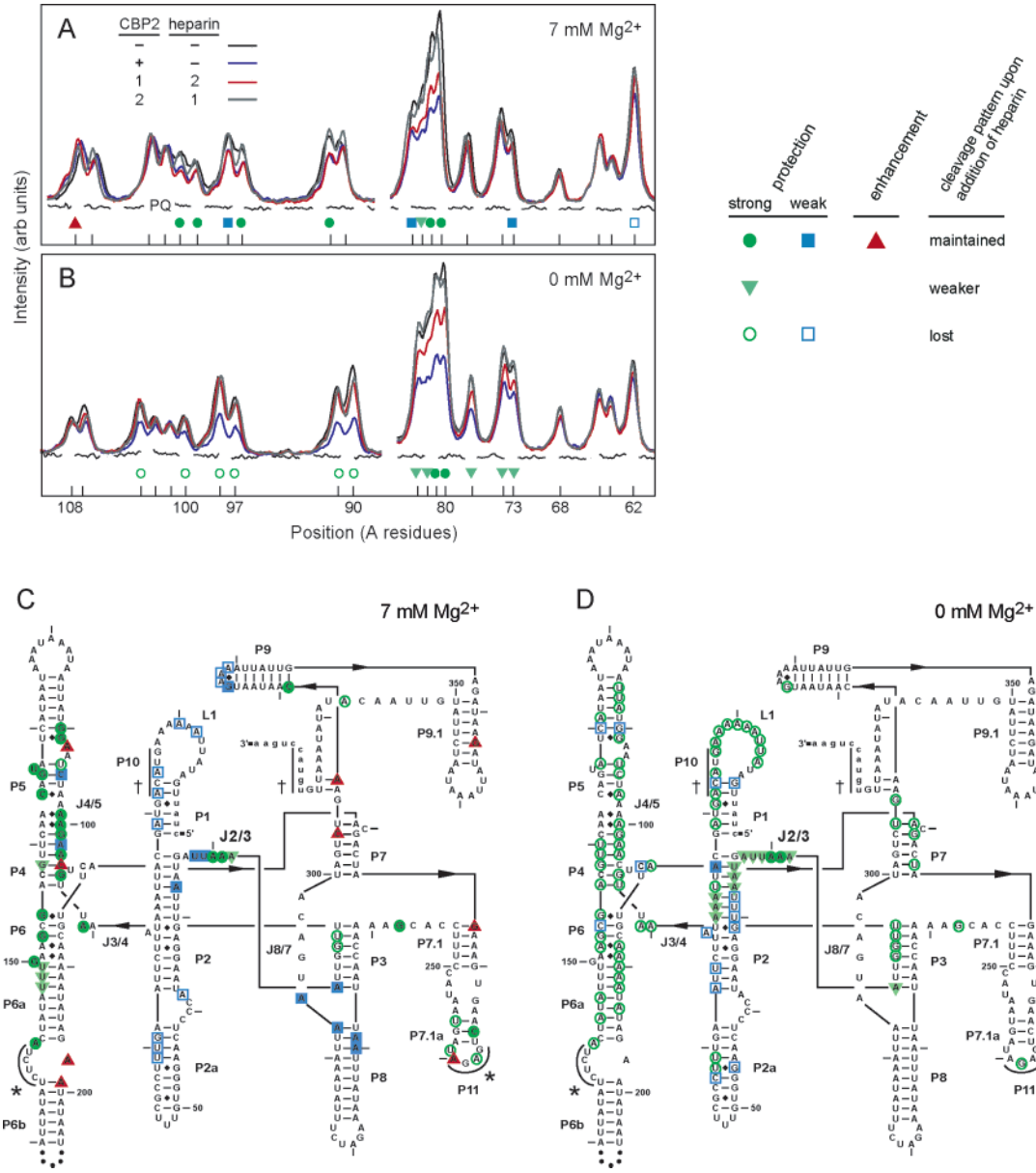


FIGURE 5: Structural consequences of CBP2 binding to the bI5 RNA collapsed and expanded states. (A, B) Representative intensity versus position plots for iodine-mediated cleavage of phosphorothioate-substituted RNAs at adenosine residues. Reactions performed in the presence and absence of CBP2 are shown with black and blue traces. The consequence of heparin addition was evaluated for complexes formed both prior to and following addition of competitor (red and gray traces). (C, D) Global summary of CBP2 binding to the collapsed and expanded state RNAs (7 and 0 mM $MgCl_2$, respectively) as monitored by iodine-mediated phosphorothioate footprinting. Symbols indicate protection and enhancement assignments (see legend); closed symbols emphasize protections retained upon addition of heparin.

P4−P6 domain, at the P3−P8 and P7.1 helices, in the P1−P2−P2a structure that comprises the 5′-domain, and in the J2/3 region (Figure 5A,C). When the complex is then treated with heparin, most regions affected by CBP2 binding remain protected (positions that retain protection in the presence of heparin are emphasized with solid symbols in Figure 5C) with the exception of the P1−P2−P2a helices. This heparin-induced structural flexibility in the 5′-domain does not, however, render the RNA inactive in splicing (Figure 4C).

The phosphorothioate footprinting pattern observed when CBP2 binds to the expanded state RNA (0 mM $MgCl_2$) differs in three distinct aspects from binding to the collapsed state. First, CBP2 binding protects a *larger* area of the RNA from cleavage, primarily in the P5−P4−P6, P1−P2−P2a, and P7−P3 helical domains (Figure 5B,D). Second and conversely, the P7.1−P7.1a structure, which constitutes a primary recognition motif for CBP2 in the native complex (*16*), is hardly protected. Last, upon addition of heparin, only a very small substructure in the RNA, specifically at P2 and J2/3, remains protected (emphasized with solid symbols in Figure 5D).

## DISCUSSION

*The Tertiary Structure Capture Mechanism Revisited.* Key features of the original tertiary structure capture model (*15*) for assembly of the bI5−CBP2 RNP are strongly supported by this and other recent (*4*, *8*) work. (i) A unimolecular RNA rearrangement is rate limiting for overall bimolecular ribonucleoprotein assembly with a non-native RNA, (ii) CBP2 does not actively fold the RNA but instead selectively recognizes (captures) the RNA native state, and (iii) the RNA dictates the overall pathway for complex assembly.

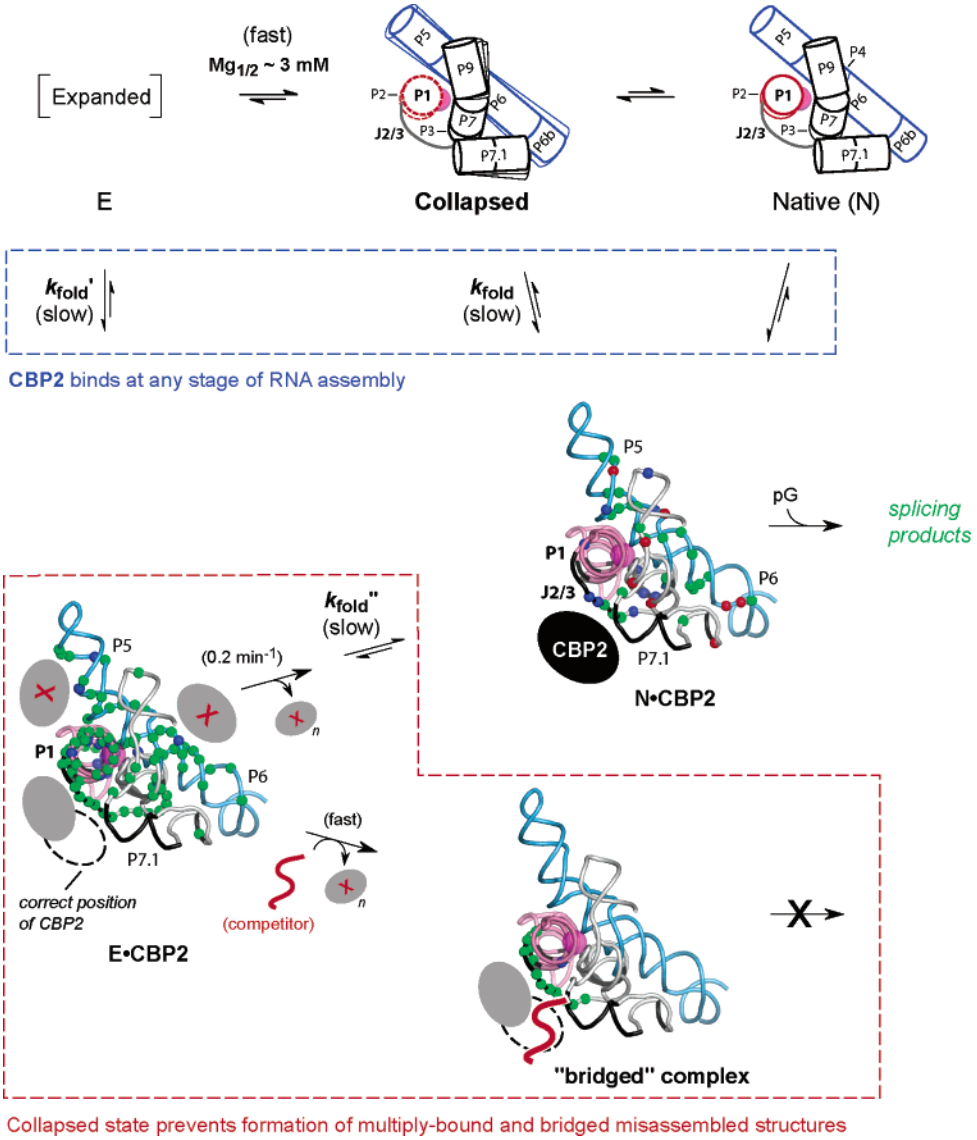


FIGURE 6: Structural basis for the self-chaperoning function of the bI5 RNA collapsed state. The splicing active site is emphasized with a magenta sphere. Correctly and incorrectly bound CBP2 is shown as a black oval or as a gray oval and red ×, respectively; a single equivalent of CBP2 that remains bound to the RNA during the rearrangement step is shown without the red ×. The correct position of CBP2 is shown with a dashed line. Strong and moderate protections from iodine-mediated phosphorothioate cleavage are shown with green and blue spheres; enhancements are in red. $k_{fold}$, $k_{fold}'$, and $k_{fold}''$ have identical (first-order) rate constants, 0.5 $min^{-1}$, within error.

However, the rate-limiting unimolecular step was originally assigned as formation of the native RNA tertiary structure (*15*) because this step is circumvented when CBP2 assembles with a correctly folded catalytic core (compare solid and open symbols in Figure 2B). We now know that CBP2 assembly with both expanded and collapsed state RNAs is governed by a distinctive unimolecular limiting step (open symbols in Figure 2B) to yield very long-lived complexes (Figure 2C).

These data support a revised version of the tertiary structure capture model in which a local conformational change, common to both collapsed and expanded states, limits overall assembly. Comparison of the RNA−CBP2 footprinting patterns obtained for complexes formed with expanded or collapsed state RNAs indicates that CBP2 binds both states stably at J2/3 (closed symbols, Figure 5C,D). J2/3 thus appears to be the key substructure that governs interaction of (is captured by) CBP2 upon assembly with the bI5 RNA.

*CBP2-Facilitated RNA Folding: Obligatory but Potentially Catastrophic.* To better illustrate the structural basis for the self-chaperoning function of the collapsed state for correct assembly of the bI5 RNP, we show the global architecture of the bI5 RNA in a useful, but unconventional, orientation, looking "down" the P1 helix (Figure 6). Helices in the free collapsed and native states are shown as cylinders, and CBP2−RNA complex-dependent footprinting protections and enhancements are shown as spheres superimposed on a ribbon model (*16*) of the intron. Strong and moderate protections are in green and blue, respectively, and enhancements are in red (Figure 6; original data are from Figure 5C,D). CBP2 binding to the near-native (*4*) collapsed state chases the RNA to the native N·CBP2 structure, which can then splice efficiently upon addition of pG. In strong contrast, binding to the expanded state RNA yields a stable but kinetically trapped, inactive, E·CBP2 complex (Figure 6).

The fundamental reason that the bI5 RNA collapsed state chaperones its own assembly is because CBP2 does not

discriminate between the collapsed and expanded states during RNP assembly (Figure 2). $k_{fold}$ and $k_{fold}'$ are identical, within error (blue dashed box in Figure 6). Two distinct misassembly events are quantitatively avoided by folding to the collapsed state: (i) inhibitory binding by multiple equivalents of CBP2 and (ii) formation of long-lived, but inactive, bridged complexes (red dashed box in Figure 6).

Misbound CBP2 in the E·CBP2 state interacts at P5, at P6, and at two independent sites in the P1−P2 structure (incorrectly bound CBP2 is shown in gray with a red × in Figure 6). Each site shares a common interaction motif consisting of approximately one turn of an RNA helix and an adjacent noncanonically paired region (Figure 5D and see E·CBP2 in Figure 6). None of these sites precisely overlaps the correct site (dashed oval in Figure 6).

Strikingly, protected surfaces in P5 and P6 are almost the *inverse* of each other in the E·CBP2 and N·CBP2 states (Figure 6). In the E·CBP2 state, protection is observed on surfaces expected to be exposed to solvent in the native complex and likely reflects misbinding by CBP2. In contrast, protection in the N·CBP2 state corresponds closely to structures located on the "inside" of the RNA or at the native CBP2−RNA interface (compare spheres in the E·CBP2 and N·CBP2 structures in Figure 6).

There are two fates for CBP2 proteins initially bound to the expanded state. Direct conversion of the E·CBP2 complex to the active N·CBP2 complex can proceed via a rearrangement mechanism. Most CBP2 equivalents dissociate from the E·CBP2 complex with a net apparent rate constant of 0.2 $min^{-1}$ (Figure 3B). A single equivalent of CBP2 (gray oval without a red × in Figure 6), however, remains bound and is able to participate in a rearrangement step characterized by a rate constant, $k_{fold}''$, of 0.5 $min^{-1}$ (see E·CBP2 to N·CBP2 pathway in Figure 6). This movement step has a rate constant similar to the unimolecular rate-limiting association step for assembly with the expanded or collapsed states (blue dashed box, Figure 6).

Alternatively, if RNA competitors are present during the rearrangement process, the kinetically trapped RNP forms a stable, but inactive, bridged complex (competitor pathway in Figure 6). Premature complex formation between CBP2 and the expanded state is catastrophic in the sense that the bridged complex is long-lived (Figure 4C). The observation that a bridged complex forms readily in the presence of a competitor also implies that the RNA binding surface of CBP2 must be formally comprised of two sites, one able to bind (incorrectly) at the J2/3 RNA structure and the other capable of interacting with a competitor (bridged complex, Figure 6).

The CBP2−bI5 RNP is likely representative of the large universe of ribonucleoprotein complexes whose RNA components achieve their correct three-dimensional shapes only upon binding by obligate protein cofactors. The dramatic change in RNA structure and interface between protein and RNA components for the E·CBP2 versus N·CBP2 complexes indicates both that the collapsed state reduces the fraction of RNA surfaces accessible for misassembly and that folding to this state can extrude misbound proteins. Given that the collapsed state profoundly limits opportunities for both correct and incorrect association of protein cofactors (Figure 6), rapid formation of this state is likely to be a central contributor to many RNP assembly reactions in complex cellular environments.

## REFERENCES


1. Buchmueller, K. L., Webb, A. E., Richardson, D. A., and Weeks, K. M. (2000) A collapsed, non-native RNA folding state, *Nat. Struct. Biol. 7*, 362−366.
2. Russell, R., Millett, I. S., Doniach, S., and Herschlag, D. (2000) Small-angle X-ray scattering reveals a compact intermediate in RNA folding, *Nat. Struct. Biol. 7*, 367−370.
3. Fang, X., Littrell, K., Yang, X., Henderson, S. J., Siefert, S., Thiyagarajan, P., Pan, T., and Sosnick, T. R. (2000) $Mg^{2+}$-dependent compaction and folding of yeast $tRNA^{Phe}$ and the catalytic domain of the *B. subtilis* RNase P RNA determined by small-angle X-ray scattering, *Biochemistry 39*, 11107−11113.
4. Buchmueller, K. L., and Weeks, K. M. (2003) Near native structure in an RNA collapsed state, *Biochemistry 42*, 13869−13878.
5. Xiao, M., Leibowitz, M. J., and Zhang, Y. (2003) Concerted folding of a Candida ribozyme into the catalytically active structure posterior to a rapid RNA compaction, *Nucleic Acids Res. 31*, 3901−3908.
6. Rangan, P., Masquida, B., Westhof, E., and Woodson, S. A. (2003) Assembly of core helices and rapid tertiary folding of a small bacterial group I ribozyme, *Proc. Natl. Acad. Sci. U.S.A. 100*, 1574−1579.
7. Su, L. J., Brenowitz, M., and Pyle, A. M. (2003) An alternative route for the folding of large RNAs: apparent two-state folding by a group II intron ribozyme, *J. Mol. Biol. 334*, 639−652.
8. Webb, A. E., and Weeks, K. M. (2001) A collapsed state functions to self-chaperone RNA folding into a native ribonucleoprotein complex, *Nat. Struct. Biol. 8*, 135−140.
9. Fang, X.-W., Thiyagarajan, P., Sosnick, T. R., and Pan, T. (2002) The rate-limiting step in the folding of a large ribozyme without kinetic traps, *Proc. Natl. Acad. Sci. U.S.A. 99*, 8518−8523.
10. Russell, R., Millett, I. S., Tate, M. W., Kwok, L. W., Nakatani, B., Gruner, S. M., Mochrie, S. G. J., Pande, V., Doniach, S., Herschlag, D., and Pollack, L. (2002) Rapid compaction during RNA folding, *Proc. Natl. Acad. Sci. U.S.A. 99*, 4266−4271.
11. Das, R., Kwok, L. W., Millett, I. S., Bai, Y., Mills, T. T., Jacob, J., Maskel, G. S., Seifert, S., Mochrie, S. G., Thiyagarajan, P., Doniach, S., Pollack, L., and Herschlag, D. (2003) The fastest global events in RNA folding: electrostatic relaxation and tertiary collapse of the Tetrahymena ribozyme, *J. Mol. Biol. 332*, 311−319.
12. Buchmueller, K. L., Richardson, D. A., and Weeks, K. M. (2002) As reported in Buchmueller, K. L., Ph.D. Dissertation, University of North Carolina at Chapel Hill.
13. Weeks, K. M., and Cech, T. R. (1995) Efficient protein-facilitated splicing of the yeast mitochondrial bI5 intron, *Biochemistry 34*, 7728−7738.
14. Garcia, I., and Weeks, K. M. (2003) Small structural costs for evolution from RNA to RNP-based catalysis, *J. Mol. Biol. 331*, 57−73.
15. Weeks, K. M., and Cech, T. R. (1996) Assembly of a ribonucleoprotein catalyst by tertiary structure capture, *Science 271*, 345−348.
16. Webb, A. E., Rose, M. A., Westhof, E., and Weeks, K. M. (2001) Protein-dependent transition states for ribonucleoprotein assembly, *J. Mol. Biol. 309*, 1087−1100.
17. Schatz, D., Leberman, R., and Eckstein, F. (1991) Interaction of *Escherichia coli* $tRNA^{Ser}$ with its cognate aminoacyl-tRNA synthetase as determined by footprinting with phosphorothioate-containing tRNA transcripts, *Proc. Natl. Acad. Sci. U.S.A. 88*, 6132−6136.
18. Rose, M. A., and Weeks, K. M. (2001) Visualizing induced fit in early assembly of the human signal recognition particle, *Nat. Struct. Biol. 8*, 515−520.


BI048626F